Hindawi
International Journal of Aerospace Engineering
Volume 2019, Article ID 3754182, 11 pages
https://doi.org/10.1155/2019/3754182

Research Article

A Three-Dimensional Guidance Logic for Continuous Curvature Path Following

Sungsu Park

Department of Aerospace Engineering, Sejong University, Seoul 05006, Republic of Korea

Correspondence should be addressed to Sungsu Park; sungsu@sejong.ac.kr

Received 12 June 2019; Accepted 11 August 2019; Published 3 September 2019

Academic Editor: Hikmat Asadov

A new simple and practical guidance logic is proposed for a vehicle to follow a general continuous curvature path defined in a three-dimensional space. The proposed guidance logic is formulated in such a way that the guidance law is to generate the command acceleration such that a vehicle pursues the designed moving virtual target, and this eventually makes a vehicle to follow a desired path. The position and velocity of the virtual target are specified explicitly by introducing the concept of the projection point and the tangentially receding distance. Numerical simulations are conducted to evaluate the precise path-following capability of the proposed guidance logic.

1. Introduction

The objective of path following is to ensure a vehicle to follow a desired path without any temporal requirements [1]. Path following is an important capability of a moving vehicle, and its relevant applications can be found in wheeled robots [1], unmanned aerial vehicles [2–5], airships [6], and spacecraft [7].

A smooth path is preferable to most moving vehicles since nonsmooth motions cannot be performed without stopping and hovering capabilities of a vehicle [8]. Although some mobile robots and flying vehicles can stop or hover at a certain point, this increases the driving or flight time and may result in degraded navigation performance. A smooth path is typically the concatenation of two primitive paths: straight-line path and circular path. Smooth transitions with continuous curvature at the junction of two primitive paths are also essential for a path to be smoothly executed by a vehicle, avoiding sudden changes in the acceleration and ensuring a smooth driving or flying [9, 10]. A continuous curvature path is generated by the path planning algorithm with consideration of both the physical constraints of a vehicle and environmental constraints [11]. The continuous curvature path planning has gained a great deal of attention, and many researchers have proposed planning algorithms, which can be found in the literatures [8–13].

Once the path is generated by a path-planning algorithm, a path-following guidance algorithm is designed for a vehicle to follow the desired path. Many path-following guidance algorithms are available in the literatures, which include the conventional proportional-integral-derivative (PID) control-based method, vector field construction method [14–16], and virtual target-based method [1, 3–5, 17–22]. A comparative study between some of path-following guidance algorithms can be found in [23]. Among them, a virtual target-based method is under consideration in this paper, and this method is positioning a moving virtual target along the desired path and using the guidance or control law to follow the virtual target. Park et al. [17, 18] and Ducard et al. [19] proposed a method in which the virtual target moves along the path at a fixed distance ahead of the vehicle, which is called the look-ahead point. However, it needs another logic to ensure the distance is long enough to intersect the desired path, and it is difficult to calculate the intersection point. Moreover, the velocity of the virtual target is not explicitly determined. Cho et al. [20] extended the concept of the look-ahead point further to the look-ahead angle and proposed a new three-dimensional nonlinear path-following

guidance law for differential geometric path. However, the look-ahead angle should satisfy several conditions, and it requires the radius of the virtual tube that envelops the entire path. Gates [21] determined the motion of the virtual target indirectly by introducing fictitious forces between the vehicle and the virtual target. However, this method generates complicated guidance command as pointed out in [22]. Typically, a virtual target method generates a nonlinear guidance law and can compensate a large deviation from the desired path. However, some methods in this approach are still for the paths in planar motion and are only applicable to primitive paths and their combinations, and the position and velocity of virtual target on a general three-dimensional path are not easy to determine. Park [24] proposed a new path-following guidance logic composed of the guidance law and the motion strategy of the virtual target. The guidance law is the combined pure proportional navigation guidance (PPNG) and pursuit guidance (PG) law, and the motion strategy explicitly specifies the motion of virtual target by introducing the concept of the projection point and the tangentially receding distance. The interesting aspect of this logic is that the virtual target is not always on the desired path. The proposed logic is simple and efficient, yet provides precise path following. However, the guidance logic was designed for only regular paths such as a straight-line, circular, and helical paths.

In this paper, a new extended guidance logic is presented for a continuous curvature path following based on our previous work [24]. The proposed guidance logic is general in the sense that it can be applied to any continuous curvature path in a three-dimensional space and includes the guidance logic proposed in [24] as a special case. Yet, it allows conceptually easy and practical way to determine the position and velocity of virtual target even when the desired path is a complicated curve and provides precise path following.

This paper is organized as follows. In the next section, a three-dimensional geometry of a continuous curvature path is presented as preliminaries to derive the proposed kinematics of a virtual target. In Section 3, the guidance law is proposed with the combined pure proportional navigation guidance (PPNG) and pursuit guidance (PG) law. In Section 4, the motion of virtual target is specified explicitly as a function of the geometry of the desired path and position and velocity vectors of the vehicle. It starts with a general continuous curvature path and moves on to special paths such as a straight-line path and a circular path. In Section 5, numerical simulations are performed to demonstrate the performance of the proposed guidance logic. Conclusions are given in Section 6.

2. Geometry of a Continuous Curvature Path

A typical parametric representation of path $\mathbf{r}_p$ in a three-dimensional space is given by [25].

$$\mathbf{r}_p(l) = x(l)\,\mathbf{i}_1 + y(l)\,\mathbf{i}_2 + z(l)\,\mathbf{i}_3, \tag{1}$$

where l is a parameter which may denote arc length, angle, or something else, and x, y, z are Cartesian components along the unit direction vectors $\mathbf{i}_1, \mathbf{i}_2, \mathbf{i}_3$ of inertial frame $\{i\}$ as illustrated in Figure 1. The use of parametric representation of a continuous curvature path is essential in deriving the proposed kinematics of a virtual target.

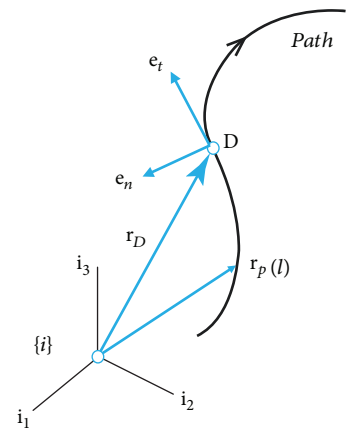

Figure 1: Parametric representation of a general path.

If $\mathbf{r}_p(l)$ is differentiable, the unit tangent vector $\mathbf{e}_t$ of a path at some point D, which is represented by $\mathbf{r}_D = \mathbf{r}_p(l_0)$, is given by

$$\mathbf{e}_t(l) = \frac{\left(d\mathbf{r}_p(l)\right)/dl}{\left|\left(d\mathbf{r}_p(l)\right)/dl\right|}, \tag{2}$$

where the derivative is evaluated at $l = l_0$, and $|\cdot|$ denotes the magnitude of a vector. The curvature κ of a path at point D is expressed in terms of the first and the second derivatives of $r_p(l)$ and is given by

$$\kappa(l) = \frac{\left|\left(\left(d\mathbf{r}_p(l)\right)/dl\right) \times \left(\left(d^2\mathbf{r}_p(l)\right)/dl^2\right)\right|}{\left|\left(d\mathbf{r}_p(l)\right)/dl\right|^3}. \tag{3}$$

For a continuous curvature path, a path-planning algorithm should generate at least a second-order differentiable path. The arc length s along a path is calculated by the following integral.

$$s = \int_0^l \left|\frac{d\mathbf{r}_p}{dl}\right| dl. \tag{4}$$

Although the actual evaluation of equation (4) is difficult in general, the use of arc length s as a parameter instead of l in equation (1) simplifies various formulas. For example, the unit tangent vector in equation (2) is simply obtained as the following form.

$$\mathbf{e}_t(s) = \frac{d\mathbf{r}_p(s)}{ds}. \tag{5}$$

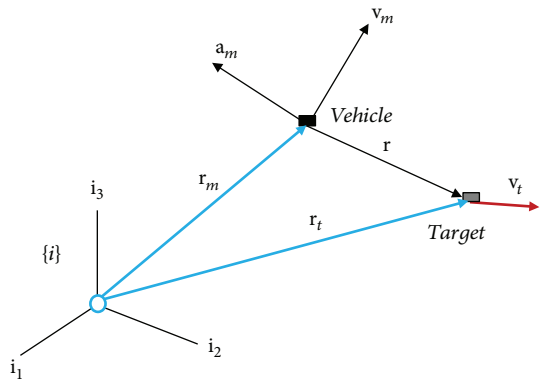

Figure 2: Pursuit geometry of the vehicle and virtual target.

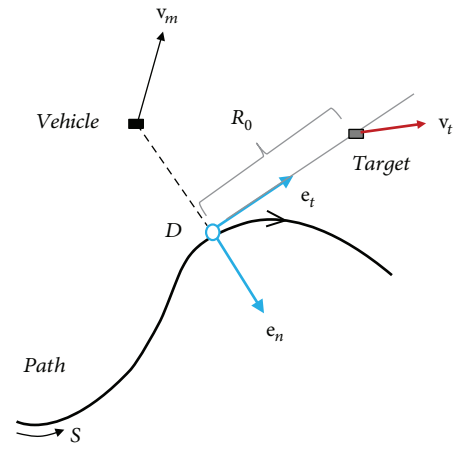

Figure 3: Continuous curvature path following.

The curvature in equation (3) is also simplified as

$$\kappa(s) = \left|\frac{d\mathbf{e}_t(s)}{ds}\right|. \tag{6}$$

Since the curvature is nonnegative by definition, it is necessary to indicate the direction to the instantaneous center of curvature at D. The unit principal normal vector $\mathbf{e}_n$ gives this direction and is defined by

$$\mathbf{e}_n(s) = \frac{(d\mathbf{e}_t(s))/ds}{|(d\mathbf{e}_t(s))/ds|} = \frac{1}{\kappa(s)}\frac{d\mathbf{e}_t(s)}{ds}. \tag{7}$$

The unit principal normal vector can be equivalently represented with parameter l as follows.

$$\mathbf{e}_n(l) = \frac{\left(\left(d^2\mathbf{r}_p(l)\right)/dl^2\right) - \left(d^2s/\mathrm{d}l^2\right)\left(\mathbf{e}_t(l)\right)}{\kappa(l)(ds/dl)^2}, \tag{8}$$

where

$$\begin{aligned}\frac{ds}{dl} &= \left|\frac{d\mathbf{r}_p(l)}{dl}\right|,\\ \frac{d^2s}{dl^2} &= \frac{\left(\left(d\mathbf{r}_p(l)\right)/dl\right)\cdot\left(\left(d^2\mathbf{r}_p(l)\right)/dl^2\right)}{ds/dl}.\end{aligned} \tag{9}$$

3. Design of Guidance Law

The proposed path-following guidance logic is composed of the guidance law and the motion strategy of virtual target. The goal of the guidance logic here is to generate the command acceleration such that a vehicle pursues the moving virtual target and eventually enables a vehicle to follow a desired path. This is an important difference compared to that of the missile guidance law in which the goal is to intercept a target.

Figure 2 illustrates the three-dimensional pursuit geometry of the vehicle and virtual target. In Figure 2, $\mathbf{r}_m$ and $\mathbf{v}_m$ denote the position and velocity vectors of the vehicle, respectively, $\mathbf{a}_m$ represents the command acceleration vector which is assumed to be perpendicular to the velocity vector of vehicle, and $\mathbf{r}$ is the relative position vector from a vehicle to the target. The position vector $\mathbf{r}_t$ and velocity vector $\mathbf{v}_t$ of the virtual target will be determined in the next section. Typically, pursuit guidance (PG) law and its variants have been used in recent path-following studies with a moving virtual target concept, because PG can direct the vehicle along the line-of-sight (LOS) irrespective of the vehicle and target velocities [3, 5]. However, in our previous work [24], the combined pure proportional navigation guidance (PPNG) and PG law was proposed as a path-following guidance law as in

$$\mathbf{a}_m = N\frac{(\mathbf{r}\times\mathbf{v})}{R^2}\times\mathbf{v}_m - hN\frac{(\mathbf{r}\times\mathbf{v}_m)}{R^2}\times\mathbf{v}_m, \tag{10}$$

where $N > 0$ and $h > 0$ are proportional and pursuit gains, respectively, R represents the distance between the vehicle and target, and $\mathbf{v} = \mathbf{v}_t - \mathbf{v}_m$ is the relative velocity vector. The first term of equation (10) is the PPNG law, and the second is the PG law. PPNG and PG laws are widely used in missile community due to their easy implementation and effectiveness [26]. PPNG keeps a constant LOS angle, and PG directs a missile along the LOS [27]. The reason for using the combined PPNG and PG is that the PPNG law can provide the instantaneous centripetal acceleration to a vehicle while the PG law can direct the vehicle along LOS in our framework of path-following guidance logic. This will be further investigated in the next section as well as roles of gain terms N and h by using a linear analysis.

4. Design of Virtual Target Motion

The proposed strategy for specifying the motion of virtual target in our previous work [24] is simple and practical. In this strategy, a virtual target is proposed to be positioned on the tangent line at the point D with a tangentially receding distance R_0 ahead of that point as illustrated in Figure 3, where the point D is the nearest projection point of a vehicle position onto the desired path. Note that the virtual target is not positioned on the path, which is the main difference between the proposed and the conventional methods.

The velocity of a virtual target is computed using the velocity of the projection point, which depends on both the velocity of vehicle and the geometry of desired path. In this paper, the desired path is assumed to be designed by a path-planning algorithm such that it satisfies the maximum curvature constraint of the vehicle considering the vehicle maneuvering limitations.

In this section, the strategy of [24] is extended to a general continuous curvature path, and the motion of virtual target is explicitly determined as a function of the geometry of the desired path and position and velocity vectors of a vehicle. It starts with a general continuous curvature path and moves on to special paths such as a straight-line path and a circular path.

4.1. General Continuous Curvature Path. The nearest projection point D of a vehicle current position onto the desired path can be computed by minimizing the following function.

$$J = \frac{1}{2}\left(\mathbf{r}_p(l) - \mathbf{r}_m\right) \cdot \left(\mathbf{r}_p(l) - \mathbf{r}_m\right). \tag{11}$$

Taking the derivative of J with respect to the parameter l and setting it to zero gives

$$0 = \frac{dJ}{dl} = \left(\mathbf{r}_p(l) - \mathbf{r}_m\right) \cdot \frac{ds}{dl}\mathbf{e}_t \tag{12}$$

or

$$0 = \frac{dJ}{dl} = \left(\mathbf{r}_p(l) - \mathbf{r}_m\right) \cdot \frac{ds}{dl}\mathbf{e}_t. \tag{13}$$

Therefore, the relative position vector from a vehicle to the nearest projection point $(\mathbf{r}_p(l) - \mathbf{r}_m)$ is perpendicular to the unit tangent vector $\mathbf{e}_t$ at the nearest projection point. To find the parameter l that minimizes the function, a gradient descent method may be used. This method starts with some initial guess of l and repeatedly performs the following update.

$$l \leftarrow l - \beta\left(\mathbf{r}_p(l) - \mathbf{r}_m\right) \cdot \frac{ds}{dl}\mathbf{e}_t, \tag{14}$$

where $\beta > 0$ is the step size. The gradient descent may take many iterations to compute a minimum value depending on the step size and initial guess of l. However, once the minimum value of l is computed with an appropriate step size, the use of this value as a new initial guess at the next iteration speeds up the computation of the nearest projection point. As an alternative to gradient descent method, Newton's method may be used for better convergence speed at the cost of more computation per each iteration.

If the parameter l^* that minimizes the function of equation (11) is found, the position vector to the nearest projection point D is given by $\mathbf{r}_D = \mathbf{r}_p(l^*)$. Then, the position vector of a virtual target is computed as follows.

$$\mathbf{r}_t(l) = \mathbf{r}_D(l) + R_0\mathbf{e}_t(l), \tag{15}$$

where l is used instead of l^* for notation simplicity. The velocity of a virtual target is the time derivative of the position vector.

$$\mathbf{v}_t(l) = \dot{\mathbf{r}}_t(l) = \frac{d\mathbf{r}_D(l)}{dl}\dot{l} + R_0\,\frac{d\mathbf{e}_t(l)}{ds}\frac{ds}{dl}\dot{l}, \tag{16}$$

where overhead dots represent the time derivative. Substituting equations (2) and (7) into (16) leads to

$$\mathbf{v}_t(l) = \frac{ds}{dl}\dot{l}\,\mathbf{e}_t + R_0\kappa\,\frac{ds}{dl}\dot{l}\,\mathbf{e}_n. \tag{17}$$

To obtain the rate of parameter $\dot{l}$, equation (13) is differentiated with respect to time.

$$\left(\frac{d\mathbf{r}_D}{dl}\,\dot{l} - \mathbf{v}_m\right) \cdot \mathbf{e}_t + \left(\mathbf{r}_D - \mathbf{r}_m\right) \cdot \frac{d\mathbf{e}_t}{dl}\,\dot{l} = 0. \tag{18}$$

Substituting equations (2) and (7) into (18) yields.

$$\dot{l} = \frac{\mathbf{v}_m \cdot \mathbf{e}_t}{(ds/dl)\left(1 + \kappa\left(\mathbf{r}_D - \mathbf{r}_m\right) \cdot \mathbf{e}_n\right)}. \tag{19}$$

To summarize, the velocity of a virtual target is given by

$$\mathbf{v}_t(l) = \frac{\mathbf{v}_m \cdot \mathbf{e}_t}{\left(1 + \kappa\left(\mathbf{r}_D - \mathbf{r}_m\right) \cdot \mathbf{e}_n\right)}\left(\mathbf{e}_t + R_0\kappa\,\mathbf{e}_n\right). \tag{20}$$

As a special case, the equilibrium state is considered. If the motion of a vehicle initially begins on the path with the direction along the unit tangent vector $\mathbf{e}_t$, i.e.,

$$\begin{aligned} \mathbf{r}_m &= \mathbf{r}_D, \\ \mathbf{v}_m &= V_m\mathbf{e}_t, \end{aligned} \tag{21}$$

then equations of target velocity vector and the relative position and velocity vectors reduce to

$$\begin{aligned} \mathbf{r} &= R_0\mathbf{e}_t, \\ \mathbf{v} &= R_0V_m\kappa\,\mathbf{e}_n, \end{aligned} \tag{22}$$

and the guidance law (10) becomes

$$\mathbf{a}_m = NV_m^2\kappa\,\mathbf{e}_n. \tag{23}$$

Therefore, with the proportional gain of $N = 1$, the guidance law produces the command acceleration that is the same to the instantaneous centripetal acceleration of a path with curvature κ. Note that pursuit guidance (PG) law generates zero command acceleration, which means that PG law makes no contribution in the equilibrium state.

The navigation gains N, h and the tangentially receding distance R_0 between the virtual target and the projection point are the design choice of the proposed guidance logic. The influence of these values can be investigated by a linear analysis similar to the method in [17, 18]. Figure 4 shows a linearization situation with assumption that the vehicle

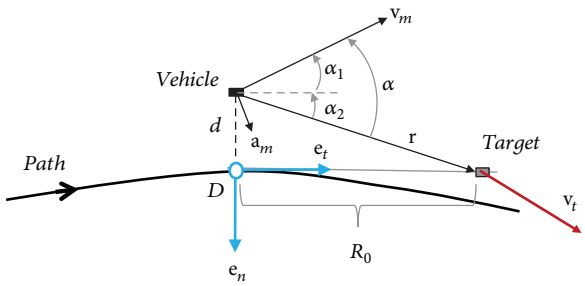

Figure 4: Linear model of continuous curvature path following.

motion is perturbed from the equilibrium state. In Figure 4, d denotes the cross-track error.

Assuming that the all vectors are almost in the same plane and the magnitudes of κd and α_1 are small, then the relative velocity vector is approximately expressed as

$$\mathbf{v} \approx V_m (R_0 \kappa + \sin \alpha_1)\, \mathbf{e}_n. \tag{24}$$

Therefore, the guidance law (10) becomes

$$\mathbf{a}_m \approx \left(N \frac{V_m^2 R_0 \kappa}{R} \cos \alpha_2 + N \frac{V_m^2}{R} \sin \alpha_1 \cos \alpha_2 + hN \frac{V_m^2}{R} \sin \alpha \right) \mathbf{e}_n. \tag{25}$$

Assuming that the magnitudes of d/R_0 and $\alpha = \alpha_1 + \alpha_2$ are small,

$$R \approx R_0, \cos \alpha_2 \approx 1, \sin (\alpha_1 + \alpha_2) \approx \frac{\dot{d}}{V_m} + \frac{d}{R_0}, \tag{26}$$

then the magnitude of command acceleration can be written as

$$a_m \approx N V_m^2 \kappa + N \frac{V_m}{R_0} \dot{d} + hN \frac{V_m}{R_0} \dot{d} + hN \frac{V_m^2}{R_0^2} d. \tag{27}$$

Equation (27) resembles a proportional and derivative (PD) control with the forcing term of $NV_m^2 \kappa$. The first two terms of the right hand side of the above equation are due to pure proportional navigation guidance (PPNG) law and the third and fourth terms pursuit guidance (PG) law. Thus, the PPNG law provides centripetal acceleration with the enhancement of the damping performance, and the PG law plays a role as a PD control. Since the vehicle is initially on the path with curvature κ in the equilibrium state and perturbed from it, $a_m \approx V_m^2 \kappa - \ddot{d}$ holds and equation (27) becomes

$$V_m^2 \kappa = N V_m^2 \kappa + \ddot{d} + N(1+h) \frac{V_m}{R_0} \dot{d} + hN \frac{V_m^2}{R_0^2} d. \tag{28}$$

Equation (28) implies that with a proportional gain of $N = 1$, the cross-track error dynamics is a second-order system and the track error eventually goes to zero. The damping ratio and natural frequency are determined by PD guidance gain and the ratio of the vehicle speed and the tangentially receding distance R_0, which are $(1+h)/2\sqrt{h}$ and $\sqrt{h} V_m / R_0$. Note that the cross-track error dynamics is at least a critically damped system.

Table 1: Summary of the proposed guidance logic.

	$\mathbf{a}_m(t) \leftarrow \text{guidance logic}(h, R_0, \mathbf{r}_p(l), \mathbf{r}_m(t), \mathbf{v}_m(t))$
1	Determine the nearest projection point $\rightarrow l^*, \mathbf{r}_D = \mathbf{r}_p(l^*)$
2	$\mathbf{e}_t = \dfrac{(d\mathbf{r}_p(l))/dl}{\lvert(d\mathbf{r}_p(l))/dl\rvert}$ at $l = l^*$
3	$\kappa = \dfrac{\lvert((d\mathbf{r}_p(l))/dl) \times ((d^2\mathbf{r}_p(l))/dl^2)\rvert}{\lvert d\mathbf{r}_p(l)/dl\rvert^3}$ at $l = l^*$
4	$\dfrac{ds}{dl} = \left\lvert \dfrac{d\mathbf{r}_p(l)}{dl} \right\rvert$ at $l = l^*$
5	$\dfrac{d^2 s}{dl^2} = \dfrac{((d\mathbf{r}_p(l))/dl) \cdot ((d^2\mathbf{r}_p(l))/dl^2)}{ds/dl}$ at $l = l^*$
6	If $\kappa = 0, \mathbf{e}_n = \mathbf{0}$ else $\mathbf{e}_n = \dfrac{((d^2\mathbf{r}_p(l))/dl^2) - (d^2 s/dl^2)\,\mathbf{e}_t}{\kappa (ds/dl)^2}$ at $l = l^*$
7	$\mathbf{r}_t = \mathbf{r}_D + R_0 \mathbf{e}_t$
8	$\mathbf{v}_t = \dfrac{\mathbf{v}_m \cdot \mathbf{e}_t}{(1 + \kappa (\mathbf{r}_D - \mathbf{r}_m) \cdot \mathbf{e}_n)} (\mathbf{e}_t + R_0 \kappa \mathbf{e}_n)$
9	$\mathbf{r} = \mathbf{r}_t - \mathbf{r}_m$
10	$\mathbf{v} = \mathbf{v}_t - \mathbf{v}_m$
11	$R^2 = \mathbf{r} \cdot \mathbf{r}$
12	$\mathbf{a}_m = \dfrac{(\mathbf{r} \times \mathbf{v})}{R^2} \times \mathbf{v}_m - h \dfrac{(\mathbf{r} \times \mathbf{v}_m)}{R^2} \times \mathbf{v}_m$

The proposed guidance logic for a general continuous curvature path following is summarized in Table 1.

In the next two subsections, the motion strategy of virtual target for a general continuous curvature path is applied to two primitive paths: straight-line path and circular path. Since geometries of these paths are simple, the resulting motions of virtual target are also simple and turn out to be the same to the ones in [24].

4.2. Special Case 1: Straight-Line Path. The straight-line path with the start position $\mathbf{r}_w$ in the direction of unit constant vector $\mathbf{e}_p$ as shown in Figure 5 can be represented parametrically as

$$\mathbf{r}_p(l) = \mathbf{r}_w + l \mathbf{e}_p, \tag{29}$$

where l is the distance along the line from $\mathbf{r}_w$. Figure 6 illustrates the pursuit geometry of the vehicle and virtual target for the straight-line path, where $\mathbf{r}_{wm} = \mathbf{r}_m - \mathbf{r}_w$ is the relative position vector of vehicle from the point W.

Then, the unit tangent vector $\mathbf{e}_t$ and unit principal normal vector $\mathbf{e}_n$ at all points on a path can be computed as follows.

$$\begin{aligned} \mathbf{e}_t(l) &= \mathbf{e}_p, \\ \mathbf{e}_n(l) &= \mathbf{0}, \end{aligned} \tag{30}$$

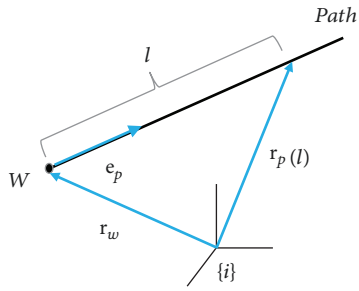

Figure 5: Parametric representation of a straight-line path.

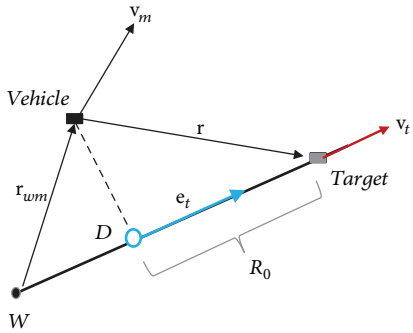

Figure 6: Straight-line path following.

and the curvature κ of a straight-line path is given by $\kappa(l) = 0$. The nearest projection point D is calculated directly from equation (13) as

$$\mathbf{r}_D = \mathbf{r}_w + (\mathbf{r}_{wm} \cdot \mathbf{e}_p)\mathbf{e}_p. \tag{31}$$

At point D, the rate of parameter $\dot{l}$ in equation (19) reduces to

$$\dot{l} = \mathbf{v}_m \cdot \mathbf{e}_p. \tag{32}$$

Therefore, the position and velocity vectors of the virtual target are simply computed as

$$\begin{aligned} \mathbf{r}_t &= \mathbf{r}_w + (\mathbf{r}_{wm} \cdot \mathbf{e}_p)\mathbf{e}_p + R_0\mathbf{e}_p, \\ \mathbf{v}_t &= (\mathbf{v}_m \cdot \mathbf{e}_p)\mathbf{e}_p, \end{aligned} \tag{33}$$

which are the same as those in [24].

4.3. Special Case 2: Circular Path. The circular path is specified by a unit vector $\mathbf{e}_{\text{rot}}$ for indicating the direction of rotation, a position vector $\mathbf{r}_c$ pointing to the center of circle, and the circle radius R_c, as shown in Figure 7. The position vector $\mathbf{r}_w$ indicates the start point of a circular path. Then, the circular path can be represented parametrically in the form as

$$\mathbf{r}_p(l) = \mathbf{r}_c + (\mathbf{r}_w - \mathbf{r}_c)\cos l + \mathbf{e}_{\text{rot}} \times (\mathbf{r}_w - \mathbf{r}_c)\sin l, \tag{34}$$

where l is the angle measured from the point W. With the use of arc length s as parameter, equation (34) becomes

$$\mathbf{r}_p(s) = \mathbf{r}_c + R_c\mathbf{e}_w \cos\frac{s}{R_c} + \mathbf{e}_{\text{rot}} \times R_c\mathbf{e}_w \sin\frac{s}{R_c}, \tag{35}$$

where $\mathbf{e}_w = (\mathbf{r}_w - \mathbf{r}_c)/R_c$.

Then, the unit tangent vector $\mathbf{e}_t$ and its derivative at a point on a circular path in terms of arc length are given by

$$\begin{aligned} \frac{d\mathbf{r}_p(s)}{ds} &= \mathbf{e}_t(s) = -\mathbf{e}_w \sin\frac{s}{R_c} - \mathbf{e}_{\text{rot}} \times \mathbf{e}_w \cos\frac{s}{R_c}, \\ \frac{d\mathbf{e}_t(s)}{ds} &= -\frac{1}{R_c}\mathbf{e}_w \cos\frac{s}{R_c} - \frac{1}{R_c}\mathbf{e}_{\text{rot}} \times \mathbf{e}_w \sin\frac{s}{R_c} \\ &= -\frac{1}{R_c^2}(\mathbf{r}_p(s) - \mathbf{r}_c). \end{aligned} \tag{36}$$

The curvature of equation (6) reduces to

$$\kappa(s) = \frac{1}{R_c}, \tag{37}$$

and the unit principal normal vector $\mathbf{e}_n$ of equation (7) becomes

$$\mathbf{e}_n(s) = -\frac{1}{R_c}(\mathbf{r}_p(s) - \mathbf{r}_c). \tag{38}$$

Figure 8 illustrates the pursuit geometry of the vehicle and virtual target for circular path, where $\mathbf{r}_{cm} = \mathbf{r}_m - \mathbf{r}_c$ is the relative position vector of vehicle from the center of circle to a vehicle.

The nearest projection point D is calculated from equation (13) as

$$\mathbf{r}_{cm} \cdot \mathbf{e}_t(s) = 0, \tag{39}$$

which occurs when

$$\frac{\mathbf{r}_{cm} - (\mathbf{r}_{cm} \cdot \mathbf{e}_{\text{rot}})\mathbf{e}_{\text{rot}}}{|\mathbf{r}_{cm} - (\mathbf{r}_{cm} \cdot \mathbf{e}_{\text{rot}})\mathbf{e}_{\text{rot}}|} = -\mathbf{e}_n(s). \tag{40}$$

Therefore, the position vector to the nearest projection point is given by

$$\mathbf{r}_D = \mathbf{r}_c + R_c\frac{\mathbf{r}_{cm} - (\mathbf{r}_{cm} \cdot \mathbf{e}_{\text{rot}})\mathbf{e}_{\text{rot}}}{|\mathbf{r}_{cm} - (\mathbf{r}_{cm} \cdot \mathbf{e}_{\text{rot}})\mathbf{e}_{\text{rot}}|}. \tag{41}$$

At point D, the rate of parameter $\dot{s}$ is computed as

$$\dot{s} = \frac{R_c(\mathbf{v}_m \cdot \mathbf{e}_t)}{|\mathbf{r}_{cm} - (\mathbf{r}_{cm} \cdot \mathbf{e}_{\text{rot}})\mathbf{e}_{\text{rot}}|}. \tag{42}$$

Substituting equations (40) and (41) into (15) yields the position vector of virtual target as

$$\mathbf{r}_t(s) = \mathbf{r}_c - R_c\mathbf{e}_n(s) + R_0\mathbf{e}_t(s). \tag{43}$$

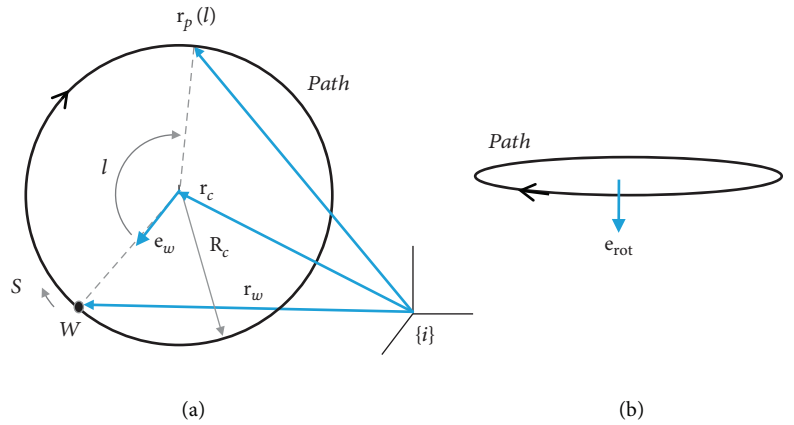

Figure 7: Parametric representation of a circular path ((a) top view, (b) side view).

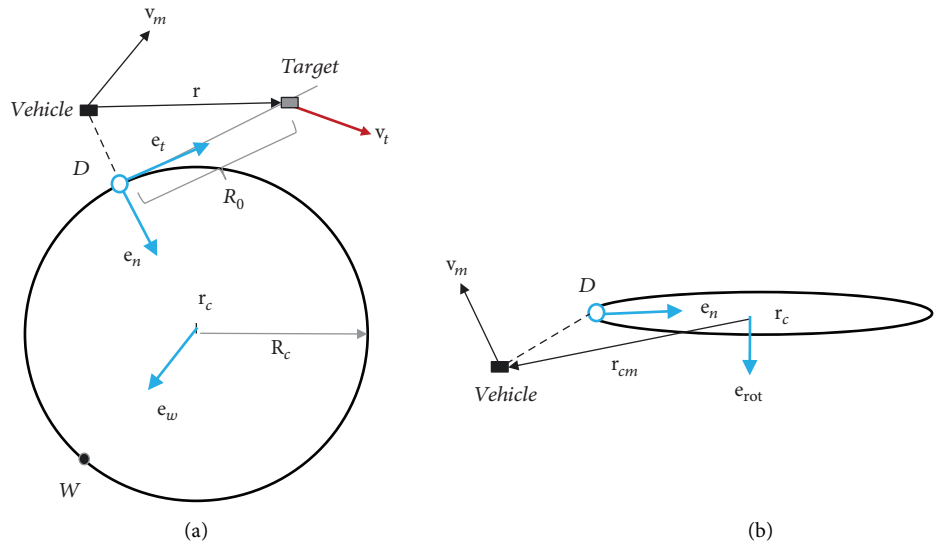

Figure 8: Circular path following ((a) top view, (b) side view).

Finally, the velocity vector of virtual target is computed by substituting equations (37) and (42) into (17).

$$\mathbf{v}_t = \frac{R_c}{|\mathbf{r}_{cm} - (\mathbf{r}_{cm} \cdot \mathbf{e}_{\text{rot}})\mathbf{e}_{\text{rot}}|}(\mathbf{v}_m \cdot \mathbf{e}_t)\mathbf{e}_t + \frac{R_0}{|\mathbf{r}_{cm} - (\mathbf{r}_{cm} \cdot \mathbf{e}_{\text{rot}})\mathbf{e}_{\text{rot}}|}\mathbf{e}_n. \tag{44}$$

Thus, the position and velocity vectors are the same those in [24].

5. Simulations

The numerical simulations are conducted to evaluate the proposed path-following guidance logic in this section. The three-dimensional path of a vehicle is assumed to be given to the vehicle a priori. The vehicle is modeled as a point mass flying at a constant speed of 20 m/sec. The tangentially receding distance R_0 is chosen as 300 m, step size $\beta = 10^{-6}$, and $N = 1$ and $h = 1$ are used in simulations.

In the simulations, two scenarios are considered and the results are shown in Figures 9–13. In the first scenario, the vehicle begins at various initial positions and poses and is supposed to fly along the helical path considered in [24]. The helical path is defined on a vertical cylinder of radius 500 m, having pitch of $L = 10(2\pi)$ m. The initial conditions used in the first scenario are summarized in Table 2. Figure 9 shows that the proposed logic can track the desired helical path without any following errors despite the large initial deviations from the path. The trajectories of cross-track error are shown in Figure 10.

As for the next scenario, a more complex path is considered as given in equation (45) to test general continuous curvature path-following capabilities of the proposed guidance logic.

$$\mathbf{r}_p(l) = 500\cos\frac{l}{10}\mathbf{i}_1 + 500\sin\frac{l}{5}\mathbf{i}_2 + \left(10\cos\frac{l}{5} + 200\right)\mathbf{i}_3\,[m]. \tag{45}$$

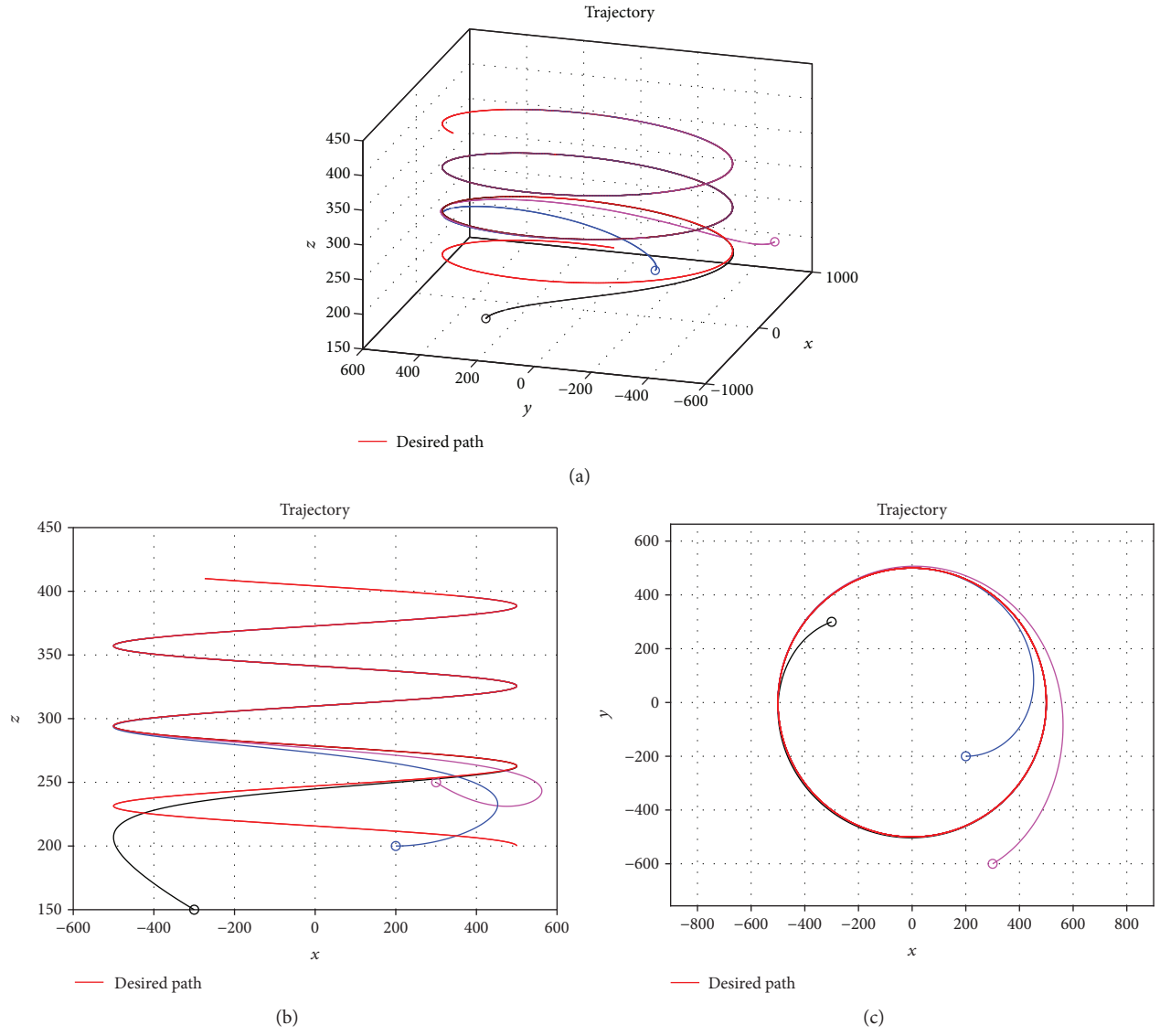

Figure 9: Helical path following. (a) Three-dimensional view, (b) side view, and (c) planar view.

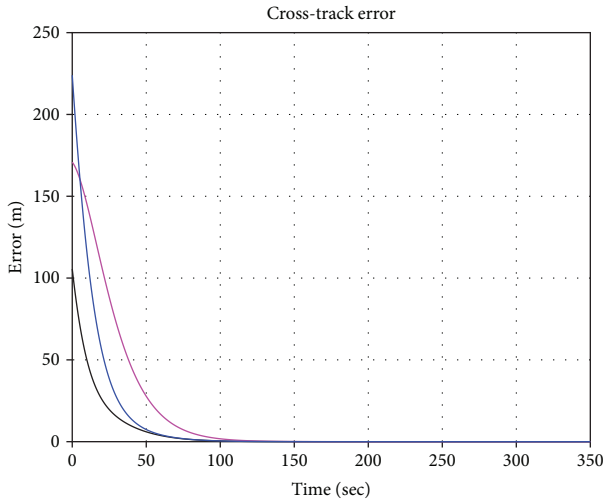

Figure 10: Cross-track errors in helical path following.

Figure 11 illustrates the defined path and its curvature as a function of parameter l. In this scenario, the vehicle begins at various initial positions and poses and is supposed to fly along the defined path. The initial conditions used in this scenario are the same to those of the first scenario as in Table 2.

Figure 12 shows how the proposed guidance logic can successfully track this path without any following error. The trajectories of cross-track error are shown in Figure 13, which verifies that all errors converge to zero as expected.

6. Conclusions

A new simple and practical guidance logic is presented for a vehicle to follow a general continuous curvature path defined in a three-dimensional space. The proposed guidance logic is general in the sense that it can be applied to any continuous curvature path and includes the guidance logic proposed in [24] as a special case.

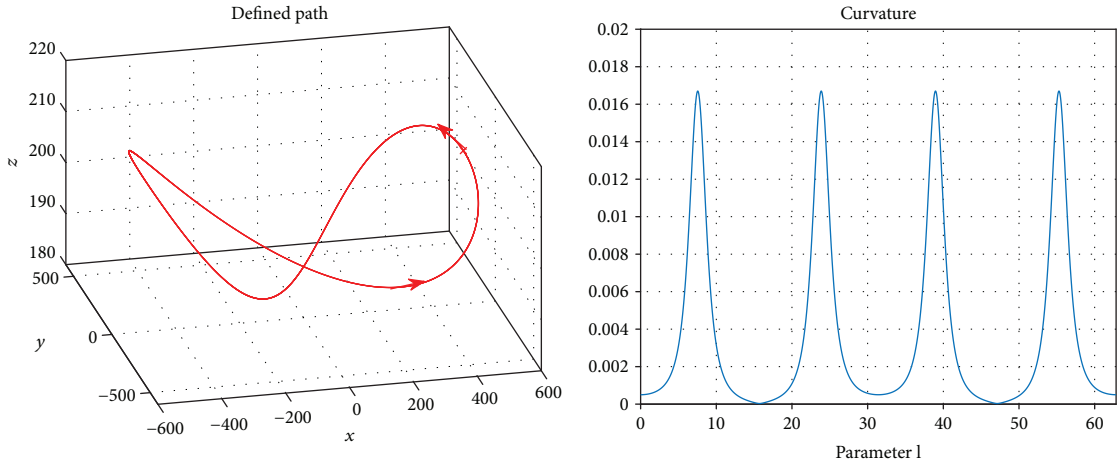

(a) (b)

Figure 11: Defined path. (a) Three-dimensional view and (b) curvature.

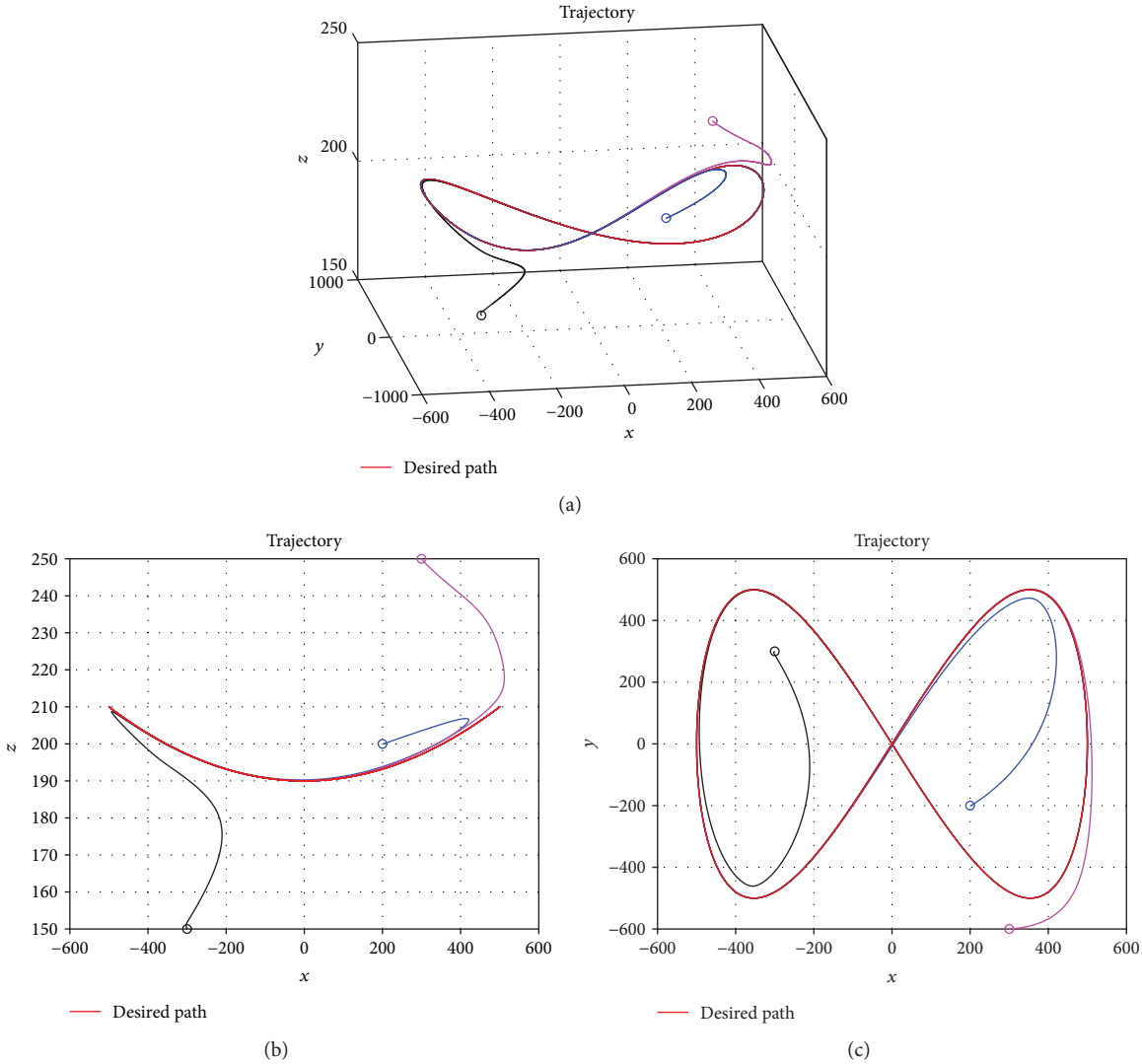

Figure 12: General path following. (a) Three-dimensional view, (b) side view, and (c) planar view.

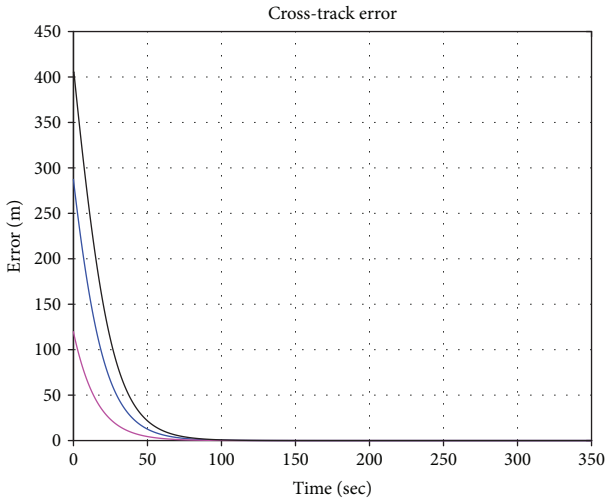

Figure 13: Cross-track errors in general path following.

Table 2: Initial conditions used in simulations.

Line colour	Initial positions (m)	Initial headings ψ and flight path angles γ (deg)
Blue	$x = 200, y = -200, z = 200$	$\psi = 0, \gamma = 0$
Magenta	$x = 300, y = -600, z = 250$	$\psi = 30, \gamma = -10$
Black	$x = -300, y = 300, z = 150$	$\psi = 200, \gamma = 10$

The proposed guidance logic is composed of the guidance law and motion strategy of the virtual target. The guidance law is a combination of the pure proportional navigation guidance (PPNG) and the pursuit guidance (PG) law, and the motion strategy explicitly specifies the motion of virtual target by introducing the concept of the projection point and the tangentially receding distance. The proposed guidance logic is formulated in such a way that the guidance law is to generate the command acceleration such that a vehicle pursues the designed moving virtual target, and this eventually makes a vehicle to follow a desired path.

The numerical simulations are conducted to evaluate the proposed path-following guidance logic. For both regular helical path and a general continuous curvature path defined in a three-dimensional space, the proposed logic shows the precise path-following capability.

Data Availability

All data used to support the findings of this study are available from the corresponding author upon request.

Conflicts of Interest

The author declares that there is no conflict of interest regarding the publication of this paper.

Acknowledgments

This research was supported by the Basic Science Research Program through the National Research Foundation of Korea (NRF) funded by the Ministry of Education (NRF-2016R1D1A1B03934475).

References

[1] D. Soetanto, L. Lapierre, and A. Pascoal, "Adaptive, non-singular path-following control of dynamic wheeled robots," in *42nd IEEE International Conference on Decision and Control (IEEE Cat. No.03CH37475)*, pp. 1765–1770, Maui, HI, USA, December 2003.

[2] Y. Hamada, T. Tsukamoto, and S. Ishimoto, "Receding horizon guidance of a small unmanned aerial vehicle for planar reference path following," *Aerospace Science and Technology*, vol. 77, pp. 129–137, 2018.

[3] E. Medagoda and P. W. Gibbens, "Synthetic-waypoint guidance algorithm for following a desired flight trajectory," *Journal of Guidance, Control, and Dynamics*, vol. 33, no. 2, pp. 601–606, 2010.

[4] V. Cichella, I. Kaminer, V. Dobrokhodov, E. Xargay, N. Hovakimyan, and A. Pascoal, "Geometric 3D path-following control for a fixed-wing UAV on SO(3)," in *AIAA Guidance, Navigation, and Control Conference*, Portland, OR, USA, August 2011.

[5] T. Yamasaki, H. Takano, and Y. Baba, "Robust path-following for UAV using pure pursuit guidance," in *Aerial Vehicles*, InTech, 2009.

[6] Z. Zuo, L. Cheng, X. Wang, and K. Sun, "Three-dimensional path-following backstepping control for an underactuated stratospheric airship," *IEEE Transactions on Aerospace and Electronic Systems*, vol. 55, no. 3, pp. 1483–1497, 2018.

[7] R. Chai, A. Savvaris, A. Tsourdos, S. Chai, and Y. Xia, "Optimal tracking guidance for aeroassisted spacecraft reconnaissance mission based on receding horizon control," *IEEE Transactions on Aerospace and Electronic Systems*, vol. 54, no. 4, pp. 1575–1588, 2018.

[8] K. Yang and S. Sukkarieh, "3D smooth path planning for a UAV in cluttered natural environments," in *2008 IEEE/RSJ International Conference on Intelligent Robots and Systems*, pp. 794–800, Nice, France, September 2008.

[9] K. Yang and S. Sukkarieh, "An analytical continuous-curvature path-smoothing algorithm," *IEEE Transactions on Robotics*, vol. 26, no. 3, pp. 561–568, 2010.

[10] J. Silva, K. Caldas, and V. Grassi Jr., "Piecewise linear continuous-curvature path planning and tracking for autonomous vehicles in crossroads," in *Simposio Brasileiro de Automacao Inteligente*, pp. 1647–1653, Campinas, SP, 2017.

[11] A. M. Lekkas, A. R. Dahl, M. Breivik, and T. I. Fossen, "Continuous-curvature path generation using Fermat's spiral, modelling," *Modeling, Identification and Control: A Norwegian Research Bulletin*, vol. 34, no. 4, pp. 183–198, 2013.

[12] V. Girbes, L. Armesto, and J. Tornero, "Continuous-curvature control of mobile robots with constrained kinematics," *IFAC Proceedings Volumes*, vol. 44, no. 1, pp. 3503–3508, 2011.

[13] J. Choi, R. Curry, and G. Elkaim, "Continuous curvature path generation based on Bezier curves for autonomous vehicles," *International Journal of Applied Mathematics*, vol. 40, no. 2, pp. 91–101, 2010.

[14] D. R. Nelson, D. B. Barber, T. W. McLain, and R. W. Beard, "Vector field path following for miniature air vehicles," *IEEE Transactions on Robotics*, vol. 23, no. 3, pp. 519–529, 2007.

[15] D. A. Lawrence, E. W. Frew, and W. J. Pisano, "Lyapunov vector fields for autonomous unmanned aircraft flight control," *Journal of Guidance, Control, and Dynamics*, vol. 31, no. 5, pp. 1220–1229, 2008.

[16] E. W. Frew and D. Lawrence, "Tracking dynamic star curves using guidance vector fields," *Journal of Guidance, Control, and Dynamics*, vol. 40, no. 6, pp. 1488–1495, 2017.

[17] S. Park, *Avionics and control system development for mid-air rendezvous of two unmanned aerial vehicles, [Ph.D. thesis]*, MIT, USA, 2004.

[18] S. Park, J. Deyst, and J. P. How, "A new nonlinear guidance logic for trajectory tracking," in *AIAA Guidance, Navigation, and Control Conference and Exhibit*, Providence, RI, USA, August 2004.

[19] G. Ducard, K. C. Kulling, and H. P. Geering, "A simple and adaptive on-line path planning system for a UAV," in *2007 Mediterranean Conference on Control & Automation*, Athens, Greece, June 2007.

[20] N. Cho, Y. Kim, and S. Park, "Three-dimensional nonlinear path-following guidance law based on differential geometry," *IFAC Proceedings Volumes*, vol. 47, no. 3, pp. 2503–2508, 2014.

[21] D. J. Gates, "Nonlinear path following method," *Journal of Guidance, Control, and Dynamics*, vol. 33, no. 2, pp. 321–332, 2010.

[22] J. Zhang, Q. Li, N. Cheng, and B. Liang, "Nonlinear path-following method for fixed-wing unmanned aerial vehicles," *Journal of Zhejiang University Science C*, vol. 14, no. 2, pp. 125–132, 2013.

[23] D. M. Xavier, B. F. N. Silva, and K. R. L. J. C. Branco, "Comparison of path-following algorithms for loiter paths of unmanned aerial vehicles," in *2018 IEEE Symposium on Computers and Communications (ISCC)*, Natal, Brazil, June 2018.

[24] S. Park, "Design of three-dimensional path following guidance logic," *International Journal of Aerospace Engineering*, vol. 2018, Article ID 9235124, 11 pages, 2018.

[25] E. Kreyszig, *Advanced Engineering Mathematics*, John Wiley & Sons, 2011.

[26] S. He, W. Wang, D. Lin, and H. Lei, "Consensus-based two-stage salvo attack guidance," *IEEE Transactions on Aerospace and Electronic Systems*, vol. 54, no. 3, pp. 1555–1566, 2018.

[27] P. Zarchan, *Tactical and Strategic Missile Guidance, Sixth Edition*, vol. 176, AIAA, 2012.